Immunization with outer membrane vesicles displaying conserved surface polysaccharide antigen elicits broadly antimicrobial antibodies

Taylor C. Stevenson[a], Colette Cywes-Bentley[b], Tyler D. Moeller[c], Kevin B. Weyant[c], David Putnam[a,c], Yung-Fu Chang[d], Bradley D. Jones[e,f], Gerald B. Pier[b], and Matthew P. DeLisa[a,c,1]

[a]Nancy E. and Peter C. Meinig School of Biomedical Engineering, Cornell University, Ithaca, NY 14853; [b]Division of Infectious Diseases, Department of Medicine, Brigham and Women's Hospital, Harvard Medical School, Boston, MA 02115; [c]Robert Frederick Smith School of Chemical and Biomolecular Engineering, Cornell University, Ithaca, NY 14853; [d]Department of Population Medicine and Diagnostic Sciences, College of Veterinary Medicine, Cornell University, Ithaca, NY 14853; [e]Department of Microbiology, University of Iowa, Iowa City, IA 52242; and [f]Genetics Program, University of Iowa, Iowa City, IA 52242

Edited by Roy Curtiss III, University of Florida, Gainesville, FL, and approved February 27, 2018 (received for review October 19, 2017)

Many microbial pathogens produce a β-(1→6)–linked poly-*N*-acetyl-D-glucosamine (PNAG) surface capsule, including bacterial, fungal, and protozoan cells. Broadly protective immune responses to this single conserved polysaccharide antigen in animals are possible but only when a deacetylated poly-*N*-acetyl-D-glucosamine (dPNAG; <30% acetate) glycoform is administered as a conjugate to a carrier protein. Unfortunately, conventional methods for natural extraction or chemical synthesis of dPNAG and its subsequent conjugation to protein carriers can be technically demanding and expensive. Here, we describe an alternative strategy for creating broadly protective vaccine candidates that involved coordinating recombinant poly-*N*-acetyl-D-glucosamine (rPNAG) biosynthesis with outer membrane vesicle (OMV) formation in laboratory strains of *Escherichia coli*. The glycosylated outer membrane vesicles (glycOMVs) released by these engineered bacteria were decorated with the PNAG glycopolymer and induced high titers of PNAG-specific IgG antibodies after immunization in mice. When a *Staphylococcus aureus* enzyme responsible for PNAG deacetylation was additionally expressed in these cells, glycOMVs were generated that elicited antibodies to both highly acetylated PNAG (∼95–100% acetate) and a chemically deacetylated dPNAG derivative (∼15% acetate). These antibodies mediated efficient in vitro killing of two distinct PNAG-positive bacterial species, namely *S. aureus* and *Francisella tularensis* subsp. *holarctica*, and mice immunized with PNAG-containing glycOMVs developed protective immunity against these unrelated pathogens. Collectively, our results reveal the potential of glycOMVs for targeting this conserved polysaccharide antigen and engendering protective immunity against the broad range of pathogens that produce surface PNAG.

oligosaccharide | glycoconjugate vaccine | immunization | infectious disease | synthetic biology

Vaccines dramatically decrease infection and illness caused by microbial and viral pathogens by inducing humoral and/or cellular immunity. In the case of pathogenic bacteria, the cell surfaces of these organisms are prominently decorated with strain-specific capsular polysaccharides (CPSs) (1) and LPSs (2), which represent excellent targets for engendering protective immunity by vaccination. However, the chemical and immunological diversities of bacterial CPS and LPS are a major impediment to their development against multiple pathogens.

One promising vaccine target with the potential to overcome the need to produce a unique carbohydrate immunogen against every microbial pathogen is the cell surface polysaccharide poly-*N*-acetyl-D-glucosamine (PNAG), a β-(1→6)–linked polymer of GlcNAc with some portion of the amino groups lacking acetate substituents. PNAG-positive organisms were initially characterized by the presence of a four-gene locus, termed intercellular adhesion (*ica*) in *Staphylococcus* (3) and polyglucosamine (*pga*) in *Escherichia coli* (4), that encodes PNAG biosynthetic enzymes. However, a recent study reported that a large number of *ica*/*pga*-negative organisms also produce PNAG, presumably by biosynthetic enzymes encoded in related but currently unidentifiable genetic loci (5). This same study identified a much broader range of PNAG-producing organisms than was originally appreciated, expanding the list to include not only additional major human bacterial pathogens but also, eukaryotic pathogens, including important fungal and protozoan parasites (5). The observation that PNAG is broadly distributed among different

Significance

A broad range of bacterial, fungal, and protozoan cells produce the surface polysaccharide poly-*N*-acetyl-D-glucosamine (PNAG), making this antigen an attractive target for vaccination against multiple human and economically important animal pathogens. While conjugate vaccines involving surface polysaccharides, such as PNAG, are a proven strategy for reducing the incidence of disease caused by bacterial pathogens, their manufacture is technically demanding, inefficient, and expensive, thereby limiting their widespread adoption. Here, we describe an alternative route to producing PNAG-containing glycoconjugates, whereby recombinant PNAG biosynthesis is coordinated with outer membrane vesicle formation in nonpathogenic *Escherichia coli* strains. The resulting glycosylated outer membrane vesicles effectively deliver PNAG antigens to the immune system while bypassing many of the drawbacks of conventional conjugate vaccines.

Author contributions: T.C.S., C.C.-B., Y.-F.C., B.D.J., G.B.P., and M.P.D. designed research; T.C.S., C.C.-B., T.D.M., K.B.W., Y.-F.C., and B.D.J. performed research; T.C.S., C.C.-B., T.D.M., K.B.W., Y.-F.C., B.D.J., G.B.P., and M.P.D. analyzed data; and T.C.S., D.P., G.B.P., and M.P.D. wrote the paper.

Conflict of interest statement: C.C.-B. is an inventor of intellectual properties (use of human mAb to PNAG and use of PNAG vaccines) that are licensed by Brigham and Women's Hospital to Alopexx Vaccine, LLC, and Alopexx Pharmaceuticals, LLC. As an inventor of intellectual properties, C.C.-B. also has the right to receive a share of licensing-related income (royalties, fees) through Brigham and Women's Hospital from Alopexx Pharmaceuticals, LLC, and Alopexx Vaccine, LLC. D.P. and M.P.D. have a financial interest in Versatope, Inc., and M.P.D. also has a financial interest in Glycobia, Inc. The interests of D.P. and M.P.D. are reviewed and managed by Cornell University in accordance with their conflict of interest policies. G.B.P. is an inventor of intellectual properties (human mAb to PNAG and PNAG vaccines) that are licensed by Brigham and Women's Hospital to Alopexx Vaccine, LLC, and Alopexx Pharmaceuticals, LLC, entities, in which G.B.P. also holds equity. As an inventor of intellectual properties, G.B.P. also has the right to receive a share of licensing-related income (royalties, fees) through Brigham and Women's Hospital from Alopexx Pharmaceuticals, LLC, and Alopexx Vaccine, LLC. The interests of G.B.P. are reviewed and managed by Brigham and Women's Hospital and Partners Healthcare in accordance with their conflict of interest policies.

This article is a PNAS Direct Submission.

[1]To whom correspondence should be addressed. Email: md255@cornell.edu.

This article contains supporting information online at www.pnas.org/lookup/suppl/doi:10.1073/pnas.1718341115/-/DCSupplemental.

Published online March 19, 2018.

microbes has led to the suggestion that numerous important human and animal pathogens could be targeted for vaccination using this single antigen.

Toward this objective, chemical conjugation of variant PNAG glycoforms to protein carriers has been performed to assess the immunogenicity and protective efficacy of these variant polysaccharides, primarily focusing on chemically modified derivatives with reduced *N*-acetylation levels. For instance, antibodies developed in response to a deacetylated poly-*N*-acetyl-D-glucosamine (dPNAG) glycoform containing only 15% *N*-acetates conjugated to the carrier protein diphtheria toxoid (DT) were found to mediate robust in vitro killing and protect animals against infection by PNAG-positive pathogens, such as *Staphylococcus aureus* (6, 7). However, opsonic and protective properties of antibodies induced by conjugates bearing PNAG with a native acetylation level (~95–100%) were inferior to the antibodies elicited by dPNAG (6). This phenomenon was most clearly illustrated using chemically defined conjugates, in which synthetic oligoglucosamines containing either 5- or 9-mer fully acetylated monosaccharides (5GlcNAc or 9GlcNAc) or 5- or 9-mer fully nonacetylated monosaccharides ($5GlcNH_2$ and $9GlcNH_2$) were coupled to the carrier protein tetanus toxoid (TT) (8) and used to immunize mice and rabbits. Consistent with earlier findings, both of the fully acetylated GlcNAc-TT conjugates elicited high titers of nonopsonic antibodies in mice, whereas both of the nonacetylated $GlcNH_2$-TT conjugates elicited highly active opsonic antibodies in mice and rabbits, with the rabbit antibodies providing excellent passive protection against *S. aureus* (8).

Despite the effectiveness of traditional conjugate vaccines (9), including those involving PNAG glycoforms, they are fraught with a number of drawbacks (10, 11). Most notably, the complex, multistep processes required for polysaccharide purification, isolation, and conjugation or for chemical synthesis are typically expensive, time consuming, and low yielding. We recently described an approach for the production of glycoconjugate vaccines that circumvents these issues by combining recombinant polysaccharide biosynthesis with outer membrane vesicle (OMV) formation in laboratory strains of *E. coli*. OMVs are naturally occurring spherical nanostructures (~20–250 nm) produced constitutively by all Gram-negative bacteria. They are composed of proteins, lipids, and glycans that originate primarily from the bacterial outer membrane and periplasm (12). OMVs are attractive as a vaccine platform, because they are nonreplicating immunogenic mimics of the producing bacteria and have natural adjuvant properties that strongly stimulate the innate and more importantly, the adaptive immune response (13–15). From a translational perspective, OMVs isolated directly from *Neisseria meningitides* have been successfully incorporated into commercial vaccine formulations for use in humans (16).

To expand the vaccine potential of OMVs, their surfaces can be remodeled with protein antigens simply by targeting expression of these foreign biomolecules to the outer membrane of an OMV-producing host strain (17–19). Such designer OMVs have been shown to stimulate strong immune responses in mice that were specific to the surface-displayed antigen (17, 19). More recently, we engineered glycosylated outer membrane vesicles (glycOMVs) that displayed recombinantly expressed carbohydrate antigens, including the polysialic acid (PSA) CPS of *N. meningitides* (20) or the *O*-antigen polysaccharide (O-PS) component of *Francisella tularensis* LPS (*Ft*-glycOMVs) (21). These glycOMVs elicited high antibody titers to their cognate polysaccharides, and mice immunized with the PSA-glycOMVs developed bactericidal antibodies against *N. meningitidis* (20), while mice receiving *Ft*-glycOMVs were protected against lethal challenge with several different strains of *F. tularensis* (21).

Here, we sought to move beyond strain-specific carbohydrate antigens by engineering glycOMVs adorned with the conserved PNAG polysaccharide for the purpose of delivering protective immunity against the broad range of pathogens that produce surface PNAG. This involved equipping a hypervesiculating strain of *E. coli*, namely JC8031 (22), with a pathway for high-level surface expression of the PNAG glycopolymer. To enrich glycOMVs with the deacetylated form of PNAG, we also heterologously expressed the *S. aureus* PNAG deacetylase IcaB in PNAG-positive JC8031 cells. The resulting strains each produced glycOMVs with exteriors that were decorated with PNAG polysaccharides that were specifically recognized by mAb F598, a human IgG1 antibody that recognizes both native PNAG and chemically prepared dPNAG (7). Mice immunized with PNAG-containing glycOMVs developed high titers of PNAG-specific antibodies, but only the glycOMVs from PNAG/IcaB-positive JC8031 cells elicited antibodies against the weakly acetylated dPNAG antigen. These latter antibodies mediated robust in vitro killing of two distinct PNAG-producing bacterial species: the Gram-positive pathogen *S. aureus* and the Gram-negative pathogen *F. tularensis* subsp. *holarctica*. In line with this killing activity, the immune responses triggered by glycOMVs were capable of protecting mice against lethal doses of *S. aureus* and *F. tularensis*, which are representative extracellular and intracellular pathogens, respectively. Taken together, these results reveal PNAG-containing glycOMVs to be a broadly effective vaccine strategy, extending across multiple bacterial species and with the added benefit of low-cost production that results from the "one-pot" biosynthesis scheme enabled by engineered bacteria.

Results

Overexpression of *pga* Operon Yields OMVs Bearing PNAG Polysaccharide. PNAG has been identified on the surface of *E. coli* K-12 strains, and its production depends on the *pgaABCD* operon (4). Here, we hypothesized that cell surface-bound PNAG would similarly decorate the exterior of OMVs released from hypervesiculating strains of *E. coli* expressing the *pgaABCD* genes (Fig. 1). To determine whether native *pgaABCD* expression was sufficient to generate OMVs adorned with PNAG, we first harvested OMVs from *E. coli* JC8031, a K-12 strain that is well-known to hypervesiculate due to deletion of the *tolRA* genes (22), and an isogenic derivative of JC8031 lacking the *pgaC* gene, which encodes a processive β-glycosyltransferase that assembles PNAG by polymerizing GlcNAc from activated UDP-GlcNAc and is essential for PNAG production (4). However, when OMVs from these strains were interrogated by dot blot analysis using mAb F598 (7), which recognizes both highly acetylated and chemically dPNAG glycoforms, no binding was observed (Fig. 2*A*). Only after very long exposure times were we able to detect PNAG in OMV fractions collected from parental JC8031 cells but not JC8031 Δ*pgaC* cells. The low abundance was directly in line with previous studies showing that wild-type bacterial strains with a single copy of the *ica*/*pga* locus produce only 1–2 fg of PNAG per cell (7, 23). In *E. coli* K-12 MG1655 cells, weak PNAG production can be overcome by mutating the gene encoding CsrA, a global regulator that posttranscriptionally represses the *pgaABCD* transcript (24). As an alternative to *csrA* disruption, we bypassed CsrA repression by overexpressing the *pgaABCD* genes from plasmid pUCP18Tc-*pga*, which contains the complete *pga* locus and can complement the defects caused by deletion of the entire *pga* operon (25). Indeed, this recombinant poly-*N*-acetyl-D-glucosamine (rPNAG) was readily detected by mAb F598 in OMV fractions isolated from JC8031 cells overexpressing plasmid-encoded *pgaABCD* (Fig. 2*A*). Digestion of rPNAG-containing OMVs with dispersin B, an extensively characterized enzyme that specifically hydrolyzes β-(1→6)–linked glucosamines (26, 27), dramatically reduced the spot intensity to nearly background (Fig. 2*A*), confirming the presence of a surface accessible β-(1→6)–linked GlcNAc polymer in these preparations. Western blot analysis of untreated rPNAG-containing OMV fractions revealed a variable degree of GlcNAc polymerization, with polymers ranging from

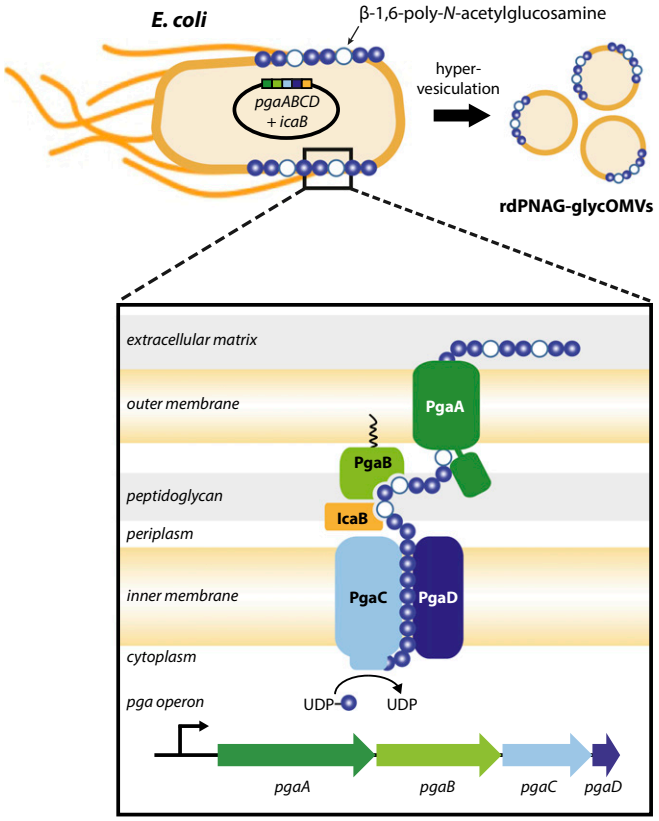

Fig. 1. Biosynthesis of glycOMVs bearing PNAG surface polysaccharide. Plasmid-based overexpression of the *E. coli pga* operon in a hyper-vesiculating strain of *E. coli* results in large quantities of rPNAG glycopolymer on the cell surface and on the corresponding OMVs shed by these cells. The native *pgaABCD* gene cluster encodes the cell envelope-spanning Pga machinery that coordinates the biosynthesis and secretion of PNAG (*Inset*). PgaC and PgaD are cytoplasmic membrane proteins that mediate PNAG polymerization, with the processive β-glycosyltransferase PgaC responsible for assembling chains of GlcNAc (blue circles) from activated UDP-GlcNAc precursor. The outer membrane porin PgaA translocates growing PNAG chains to the cell surface, while the outer membrane lipoprotein PgaB deacetylates PNAG during export, thereby introducing a limited amount of glucosamine into the polymer (white circles). Removal of additional *N*-acetyl groups is accomplished by heterologous expression of the *S. aureus* deacetylase IcaB in the periplasm, resulting in the formation of the rdPNAG glycoform. It should be noted that the occurrence of flagella, included in the drawing here, can vary from strain to strain; flagella are not present on JC8031 cells used in our studies but are likely to be found on other hyper-vesiculating strains.

~37 to >250 kDa (Fig. 2*B*). These molecular masses corresponded to roughly 100–500 GlcNAc repeats and agreed closely with an earlier report that described ~80- to 400-kDa hexosamine polymers (4). Vesicle imaging by transmission EM (TEM) revealed that the size and shape of rPNAG-containing OMVs from JC8031 cells overexpressing plasmid-encoded *pgaABCD* were indistinguishable from OMVs derived from parental JC8031 or JC8031 Δ*pgaC* cells (Fig. 2*C*), which were largely devoid of PNAG, indicating that vesicle nanostructure was largely unaffected by the presence of PNAG.

rPNAG Is Physically Associated with OMVs. Previous studies have established that the majority of PNAG produced by cells is tightly bound to the outer surface (7, 23). To determine whether rPNAG produced by our engineered *E. coli* was similarly associated with OMVs, we first performed density gradient ultracentrifugation, which leverages the fact that liposomal nanoparticles, like OMVs, are less dense than soluble macromolecules, like proteins and polysaccharides, due to their lipid content. Western blotting and Coomassie staining of the fractions obtained from density-based separation revealed that rPNAG, total proteins, and an

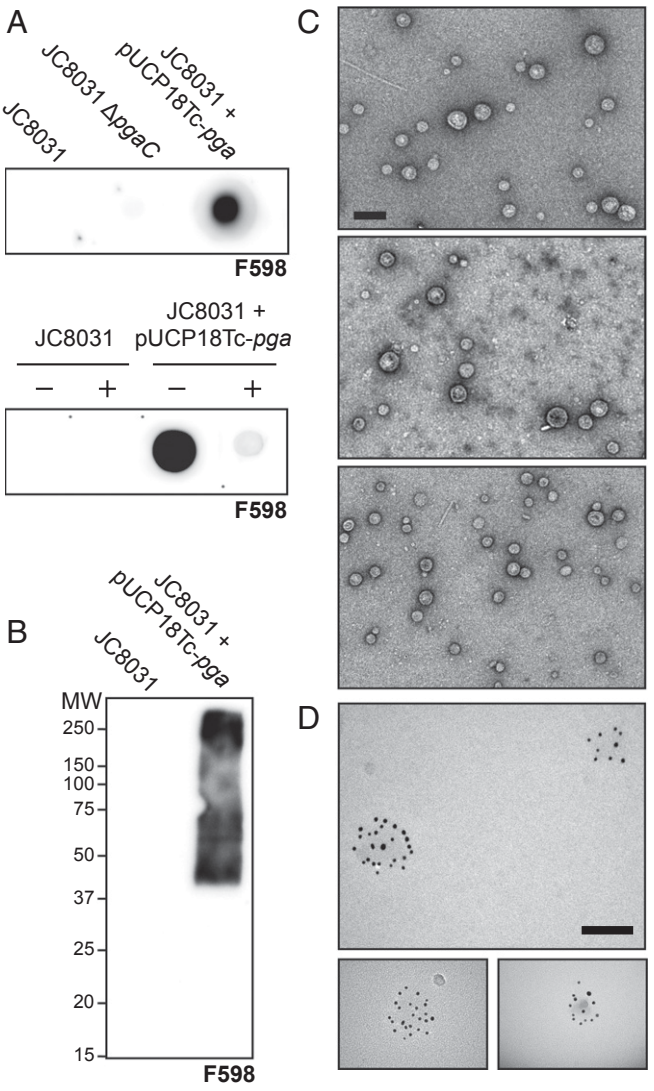

Fig. 2. Overexpression of *pgaABCD* yields PNAG-containing OMVs. (*A*) Dot blot analysis of OMV fractions derived from JC8031, JC8031 Δ*pgaC*, or JC8031 carrying plasmid pUCP18Tc-*pga* encoding the entire *pgaABCD* gene cluster (*Upper*). The same fractions from either JC8031 or JC8031 carrying pUCP18Tc-*pga* were treated with dispersin B (+) and compared with untreated (–) fractions (*Lower*). All OMV fractions were diluted 1:10 in PBS (where 1:1 dilution is 2 mg/mL of total protein), spotted on nitrocellulose membranes, and probed with mAb F598. (*B*) SDS/PAGE and Western blot analysis of OMV fractions derived from JC8031 or JC8031 carrying pUCP18Tc-*pga*. Membrane was probed with mAb F598. Molecular mass (MW) ladder is indicated on the left. (*C*) TEM analysis of OMVs produced by JC8031 (*Top*), JC8031 Δ*pgaC* (*Middle*), or JC8031 carrying pUCP18Tc-*pga* (*Bottom*). The lipid bilayers of OMVs were visualized by staining with uranyl acetate. The total protein concentration of OMVs used in this analysis was 100 μg/mL. (Scale bar: 200 nm.) (*D*) IEM analysis of OMVs derived from JC8031 carrying pUCP18Tc-*pga*. OMVs were immunostained with mAb F598 and subsequently visualized with gold-conjugated anti-human secondary. The total protein concentration of OMVs used in this analysis was 10 μg/mL. Simultaneous visualization of both the membrane and gold particles was not possible, and therefore, OMVs appear as a faint shadow on the transmission electron micrograph. (Scale bars: 100 nm.)

OMV-specific protein marker, namely OmpA, all comigrated to similar fractions (*SI Appendix*, Fig. S1), reminiscent of the gradient profiles seen previously for intact OMVs and OMV-associated cargo, including recombinantly expressed proteins and oligosaccharides (18, 20, 21, 28). To more precisely examine rPNAG localization, we performed immune-EM (IEM) using mAb F598 and a colloidal gold-conjugated anti-human secondary antibody. Whereas OMVs derived from JC8031 and JC8031 Δ*pgaC* cells failed to react with F598, JC8031 cells overexpressing plasmid-encoded *pgaABCD* exhibited strong F598 antibody labeling in circular patterns consistent with the observed diameters of OMVs (Fig. 2*D*). It should also be pointed out that there was no detectable immunostaining of these rPNAG-containing OMVs with the human IgG1 mAb F429, which has identical antibody constant regions as F598 but with variable regions that provide specific binding to the alginate antigen from *Pseudomonas aeruginosa* (29). Taken together, these results provide strong support for our hypothesis that cell surface-bound rPNAG becomes a constituent of released OMVs, giving rise to glycOMVs displaying rPNAG polysaccharides (rPNAG-glycOMVs).

Mice Vaccinated with glycOMVs Produce rPNAG-Specific Antibodies. Next, we investigated the immunogenicity and IgG isotype distribution in sera of mice receiving engineered rPNAG-glycOMVs. Female BALB/c mice immunized s.c. with rPNAG-glycOMVs developed robust IgG responses to rPNAG that increased during the weeks postimmunization (Fig. 3*A*). Maximum IgG titers were achieved 8 wk after the first immunization and were much higher than the titers measured for control mice immunized with empty OMVs or PBS (Fig. 3*A*). A similar response was observed in mice immunized with a conjugate vaccine composed of a synthetic 5-mer of fully deacetylated GlcNAc monosaccharides linked to the carrier protein tetanus toxoid ($5GlcNH_2$-TT) (8) (Fig. 3*B*). It is noteworthy that the IgG titers developed in mice immunized with an identical dose of unconjugated rPNAG were on par with the PBS control (Fig. 3*A*), consistent with the weak immunogenicity of glycans alone (9). In addition to IgGs, the rPNAG-glycOMVs also stimulated PNAG-specific IgM but not IgA antibodies (*SI Appendix*, Fig. S2*A*). It is also worth mentioning that the titers of serum antibodies against OmpA, an outer membrane protein antigen present in both empty and PNAG-containing OMV preparations, were indistinguishable (*SI Appendix*, Fig. S2*B*), confirming that an equivalent amount of OMVs was used in the immunizations.

IgG titers were further characterized by analysis of IgG1 and IgG2a titers, wherein mean IgG1 to IgG2a antibody ratios serve as an indicator of a Th1- or Th2-biased immune response. Mice immunized with rPNAG-glycOMVs or $5GlcNH_2$-TT developed titers of both rPNAG-specific IgG1 and IgG2a antibodies that were much higher than the empty OMV and PBS control groups (*SI Appendix*, Fig. S3). Interestingly, whereas $5GlcNH_2$-TT elicited a response that was strongly Th2 biased (IgG1 >> IgG2a), which is typical of most conjugate vaccines (30), including dPNAG-containing conjugates (6), the rPNAG-glycOMVs triggered a much more balanced Th1/Th2 response, which is consistent with previously reported responses to glycOMVs displaying different oligosaccharides (20, 21). Taken together, these results indicate that the display of rPNAG on the exterior of OMVs significantly increased the immunogenicity of this polysaccharide antigen.

IcaB Overexpression Augments the Immunogenicity of glycOMVs. Previous studies showed that a conjugate vaccine composed of native PNAG or dPNAG was able to stimulate production of IgG antibodies in immunized animals (6). However, immunization with the highly acetylated PNAG conjugate resulted in significantly higher antibody titers to PNAG than to dPNAG, whereas the poorly acetylated dPNAG conjugate triggered strong antibody titers to both antigens (6). This specificity is important, as the antibodies elicited by the dPNAG conjugate were superior in

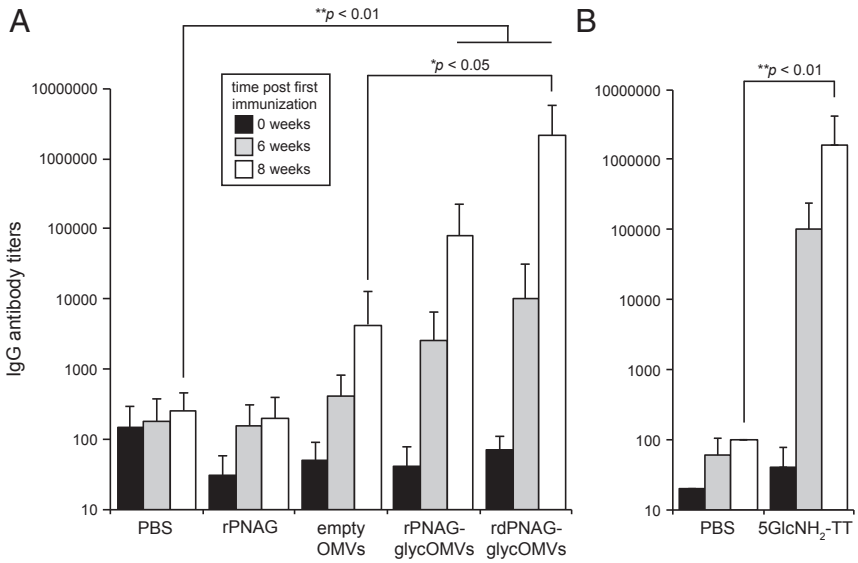

Fig. 3. Immunization with glycOMVs yields rPNAG-specific IgGs. ELISA-determined IgG antibody titers to rPNAG in sera of immunized BALB/c mice at 6 wk (gray bars) and 8 wk (white bars) after the first immunization ($t = 0$; black bars). Groups of mice ($n = 8$) were immunized as follows: (*A*) PBS, unconjugated PNAG derived from *E. coli* Top10 cells carrying pUCP18Tc-*pga* (rPNAG), OMVs from plasmid-free JC8031 Δ*pgaC* cells (empty OMVs), OMVs from JC8031 cells carrying pUCP18Tc-*pga* (rPNAG-glycOMVs), or OMVs from JC8031 carrying pUCP18Tc-*pga* and pTrc-IcaB (rdPNAG-glycOMVs); and (*B*) PBS and $5GlcNH_2$-TT conjugate. Mice immunized with OMVs were injected s.c. at $t = 0$ and boosted at 3 and 6 wk with 10 μg total protein as measured by total protein content in OMV fraction. Mice immunized with $5GlcNH_2$-TT were injected s.c. at $t = 0$ and boosted at 3 and 6 wk with 10 μg purified conjugate, which was administered with incomplete Freund's adjuvant. Purified rPNAG isolated from *E. coli* Top10 cells carrying pUCP18Tc-*pga* was used as immobilized antigen. Bars represent means, and error bars indicate SD of mean IgG titers. One-way ANOVA allowed for rejection of the null hypothesis that all immunization groups have the same mean IgG titer ($P < 0.001$). *Statistical significance ($P < 0.05$) by Tukey–Kramer honest significance difference (HSD); **Statistical significance ($P < 0.01$) by Tukey–Kramer HSD.

terms of opsonic killing activity and protective efficacy against *S. aureus* and *E. coli* infection in animals (6, 31). Here, we observed that antibodies raised to rPNAG-glycOMVs were specific for the highly acetylated PNAG as determined by measuring ELISA titers in the different sera to either native PNAG purified from *S. aureus*, having high acetylation levels, or a chemically prepared dPNAG antigen, having only a small percentage of the amino groups substituted with acetate (*SI Appendix*, Fig. S4*A*). This result was not surprising given that overexpression of *pgaABCD* in *E. coli* gives rise to a PNAG glycopolymer that contains only about 3% dPNAG (4).

In an effort to increase PNAG deacetylation in glycOMVs, *E. coli* cells carrying the rPNAG-producing plasmid pUCP18Tc-*pga* were cotransformed with a second plasmid for heterologously expressing the PNAG deacetylase, IcaB, from *S. aureus*. Whereas the *E. coli* deacetylase, PgaB, is a lipoprotein, the IcaB enzyme is membrane associated through binding to peptidoglycan (7). To facilitate IcaB expression in *E. coli*, we removed its native secretion signal and replaced it with an *E. coli* Sec-dependent signal peptide for high-level periplasmic expression. Western blot analysis of both periplasmic and whole-cell fractions derived from this strain showed that IcaB was present as a soluble protein in the periplasm and that the majority of it was associated with the membrane containing whole-cell fraction (*SI Appendix*, Fig. S5*A*). Importantly, OMVs isolated from cells overexpressing *pgaABCD* and *icaB* [recombinant deacetylated poly-*N*-acetyl-D-glucosamine (rdPNAG)-glycOMVs] were recognized by mAb F598 to an extent that was indistinguishable from that observed for rPNAG-glycOMVs (*SI Appendix*, Fig. S5*B*), indicating that these OMVs were similarly decorated with PNAG. Unfortunately, chemical characterization using GC/MS or NMR on preparations obtained from these bacteria was unsuccessful, a well-documented problem (5) that prevented us from definitively confirming the degree of deacetylation for PNAG produced in IcaB-expressing cells. Underlying the barrier to chemical characterization of PNAG is the finding that, unlike bacterial CPSs that can be readily isolated from culture supernatants and microbial cell surfaces, almost all of the PNAG is tightly bound to the cell surface and thus, must be extracted for purification (7, 23). As a result, the actual yields are markedly reduced by the difficulty in extracting PNAG from the cell surface as well as additional significant losses caused by the insolubility of PNAG at neutral pH and the complex purification procedures needed to eliminate tightly associated contaminating bacterial antigens (6, 23). Nonetheless, indirect evidence for increased deacetylation was obtained from immunization experiments. First, the rPNAG antigen-specific antibody titers developed in mice immunized with rdPNAG-glycOMVs were significantly higher than those obtained with rPNAG-glycOMVs, rivaling the titers observed for immunization with the $5GlcNH_2$-TT conjugate (Fig. 3). Second, antibodies in mice immunized with rdPNAG-glycOMVs were directed to epitopes on both highly and poorly acetylated PNAG antigens, which was in stark contrast to the rPNAG-glycOMV–induced antibodies that mainly reacted with acetyl-containing epitopes (*SI Appendix*, Fig. S4*A*). It is also noteworthy that the rdPNAG-glycOMVs stimulated PNAG-specific IgM antibodies and unlike the more acetylated rPNAG-glycOMVs, IgA antibodies as well (*SI Appendix*, Fig. S2*A*).

Detoxified glycOMVs Retain Immunogenicity. One concern with the use of bacterial OMVs as a vaccination platform is the reactogenicity caused by the presence of LPS on the membrane surface. To circumvent this issue, we previously remodeled the lipid A structure of *E. coli* strain JC8031 at the genetic level by knocking out the acyl transferase, LpxM, which causes the strain to produce a pentaacylated form of lipid A that has significantly reduced toxicity (32). The resulting strain, JH8033, yielded OMVs that were significantly less toxic as measured by hTLR4 activation, while retaining full immunostimulatory qualities (21). OMVs harvested from JH8033 cells overexpressing *pgaABCD* and *icaB* reacted strongly with mAb F598 (*SI Appendix*, Fig. S5*B*), indicating that the abundance of rPNAG on the exterior of OMVs was not diminished by remodeling of lipid A. Importantly, the IgG antibody titers developed in mice immunized with rdPNAG-glycOMVs harboring wild-type lipid A vs. remodeled lipid A were nearly identical (*SI Appendix*, Fig. S4*B*), indicating that reducing the reactogenicity by lipid A modification does not adversely affect the immunogenicity of rPNAG-containing glycOMVs.

Opsonic Killing Activity of glycOMV-Induced Antibodies Against *S. aureus*. Encouraged by the robust polysaccharide-specific IgG responses induced by glycOMVs, we next screened mouse sera for opsonic killing activity in the presence of human polymorphonuclear leukocytes (PMNs) and autologous human complement. While PNAG is known to be present on the surfaces of many important Gram-negative and Gram-positive bacterial pathogens (5), we focused initially on *S. aureus*, because PNAG production is most extensively characterized in this bacterium. Mice immunized with rdPNAG-glycOMVs clearly had opsonically active antibodies that mediated killing of *S. aureus* CP8 strain MN8, whereas mice receiving empty OMVs or PBS had significantly less killing activity (Fig. 4*A*). It is noteworthy that the opsonic killing activity measured for these antibodies exceeded that of the serum antibodies developed in mice immunized with the $5GlcNH_2$-TT conjugate and was on par with that measured for the positive control mAb F598 (Fig. 4*A*). Importantly, there was no significant bactericidal activity observed when key components of the assay were missing or inactive (Fig. 4*A*).

Protective Efficacy of glycOMVs Against *S. aureus* Challenge in Mice. To determine whether the opsonic killing activity measured above translated to a protective immune response in animals, immunized BALB/c mice were challenged at 56 d after the initial dose with 10 times the modified LD_{50} (mLD_{50}) of *S. aureus* strain Rosenbach via tail vein injection. Mice immunized with rdPNAG-glycOMVs or their detoxified counterpart had the highest survival rates (~60%), while the survival rates of those receiving the $5GlcNH_2$-TT conjugate were slightly lower (42%). That there was no significant difference in survival between the two rdPNAG-containing OMV-treated groups indicates that lipid A remodeling can effectively reduce the reactogenicity of PNAG-containing OMV candidates without compromising their protective activity. As expected, mice immunized with PBS or empty OMVs had the lowest survival rates (<20%) (Fig. 4*B*). Importantly, these survival rates correlated strongly with the measured PNAG-specific IgG titers and opsonic killing activity developed in these mice. It is also noteworthy that rPNAG-glycOMVs, which putatively contained mostly acetylated PNAG as discussed above, afforded a level of protection that was on par with the $5GlcNH_2$-TT conjugate, which was completely deacetylated. This result was particularly interesting, because previous studies have shown that passive administration of antibodies raised against the highly acetylated, native PNAG antigen is unable to mediate clearance of *S. aureus* from the blood or protect against a high-dose lethal infection (6, 8).

Serum Bactericidal Activity of glycOMV-Induced Antibodies Against *F. tularensis*. In light of the fact that diverse Gram-negative and Gram-positive bacterial pathogens produce surface-bound PNAG (5), we sought to determine whether PNAG-containing OMVs could provide cross-species protection. We focused our attention on *F. tularensis*, a Gram-negative, nonspore-forming bacterium and the causative agent of tularemia, which had not previously been confirmed for surface-associated PNAG production. Our own genetic analysis of published genomes failed to

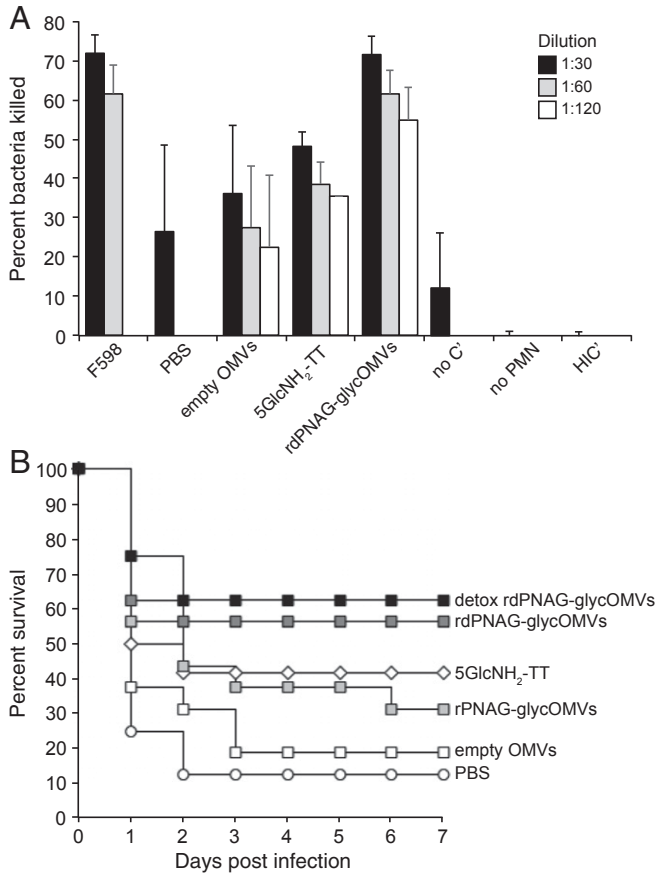

Fig. 4. glycOMVs elicit opsonically active antibodies and protective immune responses against *S. aureus*. (*A*) Opsonic killing activity against *S. aureus* CP8 strain MN8 by different dilutions of serum from BALB/c mice ($n = 8$ except for $5GlcNH_2$-TT, where $n = 4$) immunized with PBS, empty OMVs, rdPNAG-glycOMVs, or $5GlcNH_2$-TT. Bars represent means, and error bars indicate SD of the mean. The mAb F598 served as positive control and was tested at 10 μg/mL (black bars) and 5 μg/mL (gray bars). The mAb F429, which is specific for the *P. aeruginosa* alginate antigen, was tested at 10 μg/mL and served as a negative control to which all data were normalized. Negative control serum from mice receiving PBS was only tested at a dilution of 1:30. All of the sera were tested in the absence of either human PMNs (no PMNs) or human complement (no C′) or in the presence of heat-inactivated complement (HIC′), and the average of this entire dataset is shown. (*B*) Kaplan–Meier survival analysis of groups of BALB/c mice ($n = 16$ except for $5GlcNH_2$-TT, where $n = 12$, and both detoxified OMV groups, where $n = 8$) that were immunized with PBS, empty OMVs, rPNAG-glycOMVs, rdPNAG-glycOMVs, detoxified rdPNAG-glycOMVs, or $5GlcNH_2$-TT and subsequently challenged at 56 d after the first immunization with 1×10^9 cfu/mL ($10 \times mLD_{50}$) of *S. aureus* strain Rosenbach in 200 μL sterile PBS via tail vein injection. Mice immunized with OMVs were injected s.c. at $t = 0$ and boosted at 3 and 6 wk with 10 μg total protein as measured by total protein content in the OMV fraction. Mice immunized with $5GlcNH_2$-TT were injected s.c. at $t = 0$ and boosted at 3 and 6 wk with 10 μg purified conjugate, which was administered with incomplete Freund's adjuvant. The groups receiving rdPNAG-glycOMVs and detoxified rdPNAG-glycOMVs showed statistically significant protection over the PBS group ($P < 0.05$) as determined by a log rank test.

identify genetic loci in *F. tularensis* similar to the known four-gene *ica* or *pga* loci in *S. aureus* and *E. coli*, respectively; however, a number of *ica*/*pga*-negative organisms have been confirmed to produce PNAG by biosynthetic enzymes encoded in related but currently unidentifiable genetic loci (5). Therefore, we proceeded to experimentally interrogate the surface of the *F. tularensis* subsp. *holarctica* live vaccine strain (LVS) for PNAG expression using a sensitive and specific immunochemical fluorescence analysis developed previously (5). Indeed, PNAG was detected by confocal microscopy on the surface of *F. tularensis* LVS cells using mAb F598 directly conjugated to AlexaFluor 488 (green fluorescence) (*SI Appendix*, Fig. S6). To confirm that mAb F598 was binding to PNAG, cells were subjected to digestion with the PNAG-degrading enzyme dispersin B or a related degradative control enzyme, chitinase, that specifically hydrolyzes the β-(1→4)–linked GlcNAc chitin molecule or were instead treated with sodium metaperiodate. Chitinase-resistant but dispersin B- and periodate-sensitive binding of mAb F598 was observed, thereby showing PNAG-specific labeling of cells (*SI Appendix*, Fig. S6). Nearly identical immunochemical labeling results were observed for two additional subspecies of *F. tularensis*, namely *F. tularensis* subsp. *novicida* U112 and *F. tularensis* subsp. *tularensis* strain Schu S4 (*SI Appendix*, Fig. S7).

Next, we investigated *F. tularensis* killing activity using a serum bactericidal assay (SBA). The serum antibodies developed in mice immunized with rdPNAG-glycOMVs exhibited potent concentration-dependent bactericidal activity against *F. tularensis* LVS that rivaled the activity measured for serum antibodies induced by the $5GlcNH_2$-TT conjugate or the positive control mAb F598 (Fig. 5*A*). It should be noted, however, that mice immunized with $5GlcNH_2$-TT had highly variable bactericidal activity, with antibodies from sera from two mice showing virtually no bactericidal activity and antibodies from sera from two others showing complete killing at all concentrations tested. Importantly, mice receiving PBS generated little to no bactericidal activity above the background measured in control tubes that contained bacteria but lacked complement or included heat-inactivated complement, whereas mice receiving empty OMVs showed a moderate level of bactericidal activity under the conditions tested (Fig. 5*A*). This latter activity was unexpected and indicated that some of the antibodies raised to features present in the empty OMVs were cross-reactive with *F. tularensis* LVS.

Protective Efficacy of glycOMVs Against *F. tularensis* LVS Challenge in Mice. We next investigated whether PNAG-containing OMVs could engender protective immunity against lethal *F. tularensis* challenge. Our focus here was on detoxified rdPNAG-glycOMVs because of the protection that was observed above for this vaccine candidate against *S. aureus* challenge. At 70 d after the initial dose, immunized mice were challenged with 500 cfu *F. tularensis* LVS, which in BALB/c mice, has an LD_{50} of ∼1 cfu when administered by i.p. injection (33). Here, all PBS-treated and empty OMV-treated control mice died within a week when infected i.p. with ∼500 times the LD_{50} of LVS (Fig. 5*B*), similar to our previous observations (21). In contrast, all but one of the mice immunized with detoxified rdPNAG-glycOMVs containing remodeled lipid A were completely protected against the same lethal dose of LVS (Fig. 5*B*). Not only did we observe excellent protection, but the surviving rdPNAG-glycOMV–vaccinated mice did not even appear sick, suggesting that protection was probably higher than we were able to see in this experiment. Consistent with the SBA results above, the $5GlcNH_2$-TT conjugate also afforded some protection, although the effect of this vaccine candidate was more variable, with one mouse succumbing by day 7 and two additional mice that appeared quite sick dying by day 8 (Fig. 5*B*). Taken together, our results are indicative of the potential of rdPNAG-glycOMVs to serve as a uniquely broad spectrum vaccine for inducing immunity against diverse bacterial pathogens.

Discussion

The development of PNAG-based vaccines has been an ongoing activity ever since the discovery of this bacterial surface polysaccharide. To overcome the fairly high doses (100 μg per animal) of purified PNAG that were required to evoke antibodies in mice (34), many efforts have focused on chemically conjugating acetylated and deacetylated glycoforms of PNAG to carrier

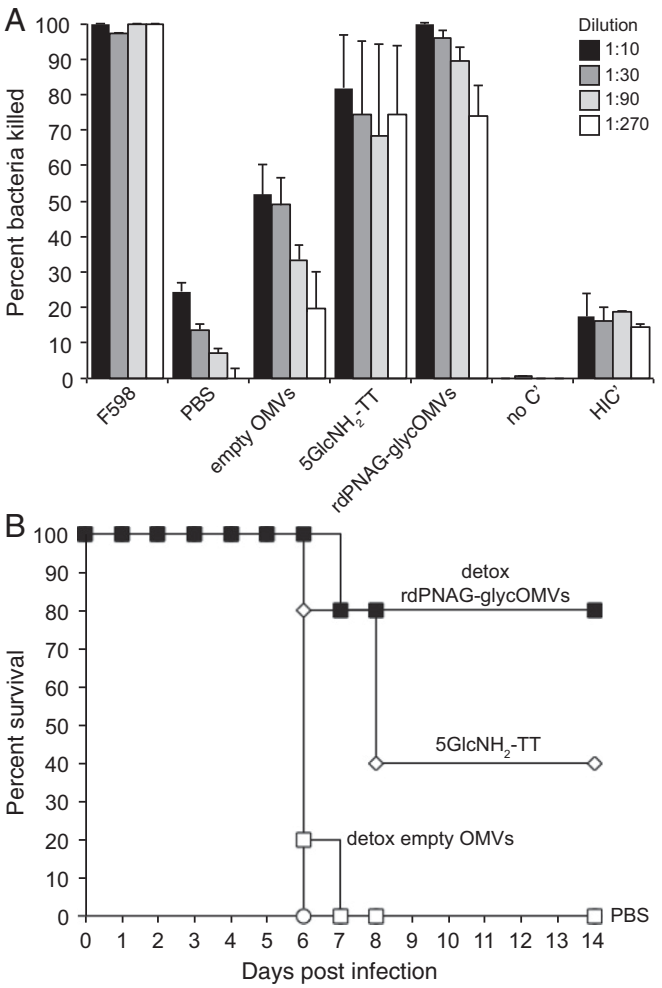

Fig. 5. GlycOMVs elicit bactericidal antibodies and protective immunity against *F. tularensis* LVS. (*A*) Serum bactericidal activity against *F. tularensis* LVS by antibodies in the serum of BALB/c mice ($n = 8$ except for $5GlcNH_2$-TT, where $n = 4$) immunized with PBS, empty OMVs, rdPNAG-glycOMVs, or $5GlcNH_2$-TT. Survival data are derived from standard SBA, where dilutions of serum from immunized mice were tested against *F. tularensis* LVS Iowa in the presence of baby rabbit complement. All data were normalized to the killing measured for baby rabbit complement alone. Bars represent means, and error bars indicate SD of the mean. The mAb F598 served as positive control and was assayed according to the same dilution scheme, with 1:1 being equivalent to 1 mg/mL. Negative controls included mAb F598 in the absence of human complement (no C′) or in the presence of heat-inactivated complement (HIC′). (*B*) Kaplan–Meier survival analysis of groups of BALB/c mice ($n = 5$) that were immunized with PBS, detoxified empty OMVs, detoxified rdPNAG-glycOMVs, or $5GlcNH_2$-TT and subsequently challenged at 70 d after the first immunization with *F. tularensis* LVS Iowa via i.p. injection of 500 cfu ($\sim 500 \times LD_{50}$). Mice immunized with OMVs were injected s.c. at $t = 0$ and boosted at 2 and 4 wk with 10 μg total protein as measured by total protein content in OMV fraction. Mice immunized with $5GlcNH_2$-TT were injected s.c. at $t = 0$ and boosted at 2 and 4 wk with 10 μg purified conjugate, which was administered with incomplete Freund's adjuvant. The groups receiving detoxified rdPNAG-glycOMVs showed statistically significant protection over the PBS and detoxified empty OMV groups ($P < 0.05$) as determined by a log rank test. The $5GlcNH_2$-TT group was not significantly higher than the PBS group or significantly lower than the detoxified rdPNAG-glycOMVs group.

proteins, such as DT or TT (5, 6, 8), which is a common technique for enhancing the immunogenicity and effectiveness of polysaccharide antigens (9). Collectively, these studies and other related studies have revealed the potential of PNAG to serve as a unique and broad spectrum vaccine antigen. Unfortunately, despite their ability to create long-lasting immune responses against bacteria (9), conjugate vaccine production is hampered by a number of well-documented drawbacks (10, 11). For example, the traditional route for producing prototypical conjugates involves complex synthetic chemistry for isolating, activating, and coupling the polysaccharides to protein carriers. Because the carbohydrate antigens are usually sourced from pathogenic organisms, yields can be low due to difficulties culturing certain microbes to high densities, and production can be hazardous, which may necessitate higher biosafety levels. The chemical treatment steps used to purify carbohydrate antigens and cross-link them to proteins can destroy acid-labile sugars and are often not reproducible, resulting in inconsistent products with batch-to-batch variability.

Here, we sought to engender broadly protective immunity by targeting PNAG with an alternatively prepared vaccine candidate, the production of which overcomes the low yields, high costs, batch-to-batch variability, and slow development timelines of conventional conjugate vaccines. This feat was achieved by coordinating rPNAG biosynthesis with OMV formation in nonpathogenic strains of *E. coli*. Our strategy was inspired in part by previous findings that remodeling the surface of OMVs with CPS or LPS antigens—including the *N. meningitidis* serogroup B PSA capsule (20), the *Streptococcus pneumoniae* serotype 14 capsule (35), and the O-PS portion of LPS from *F. tularensis* Schu S4 (21)—yielded OMV-based vaccine candidates called glycOMVs that significantly boosted antigen-specific IgG levels in mice. In all cases tested, glycOMVs triggered the production of serum bactericidal or opsonic antibodies, and they were able to protect mice against pathogen challenge (20, 21, 35). Likewise, glycOMVs that displayed rPNAG on their exterior elicited antibodies that mediated efficient in vitro killing of *S. aureus* CP8 strain MN8 and *F. tularensis* subsp. *holarctica* LVS Iowa, and mice receiving glycOMV vaccine candidates developed protective immunity against these bacterial species. In light of the well-established physical association for PNAG (7, 23), it is important to point out that a number of studies have proven that noncovalent association between an oligosaccharide and carrier molecule is sufficient to elicit robust immune responses (36, 37). Moreover, the fact that all normal human sera analyzed to date have good titers of natural but nonprotective antibody to PNAG based on exposure to normal flora (38) further indicates that the molecule is immunogenic when intercalated into the bacterial membrane or outer surface. Hence, the protective immunity that we observed with noncovalently attached PNAG on the exterior of OMVs provides further support of this phenomenon.

Consistent with earlier findings discussed above, glycOMVs bearing the less acetylated rdPNAG (generated by IcaB coexpression) induced serum antibodies that recognized both native PNAG and dPNAG and were more immunogenic and protective than their highly acetylated rPNAG-glycOMVs counterparts. In fact, the serum IgG antibody levels rivaled those induced by $5GlcNH_2$-TT, and the protection afforded by the rdPNAG-glycOMVs was better than with the conjugate. While the underlying reasons for this superior performance are currently unknown, one possibility is the balanced Th1/Th2 humoral response triggered by glycOMVs compared with the strongly Th2-biased response to $5GlcNH_2$-TT. In fact, the relatively high IgG2a levels developed in BALB/c mice receiving glycOMVs are quite remarkable when one considers that this mouse strain tends to develop a Th2-predominant immune response. While a Th1-biased immune response is generally considered to be important for intracellular pathogens, such as *F. tularensis*, and a Th2-biased response is generally considered to be important for extracellular pathogens, like *S. aureus*, mounting evidence highlights the importance of more comprehensive immune mechanisms (i.e., Th1, Th2, Th17) for the two pathogens that were targeted here (39–41) and could help to explain the

effectiveness of glycOMVs in conferring protection. Additional explanation for the effectiveness of OMV-based vaccines may come from their ability to activate innate signaling pathways. As OMVs are immunological snapshots of the outer membranes and periplasms of the *E. coli* cells from which they are derived, they contain many pathogen-associated molecular patterns that stimulate different Toll-like receptors (TLRs). For example, the peptidoglycan and lipoproteins in OMVs likely function as TLR2 agonists, and lipid A likely functions as a TLR4 agonist (42). It is also worth mentioning that glycOMVs displaying the rPNAG glycoform were able to confer some level of protection against *S. aureus*, suggesting that the previously observed self-adjuventicity of OMVs (17, 19) may help to overcome the poor protective efficacy of highly acetylated PNAG. Nonetheless, the superior immunogenicity and protective efficacy of the less acetylated rdPNAG-glycOMVs suggest that this is the more tractable formulation to pursue for vaccine development. In fact, additional deacetylation of the rdPNAG-glycOMVs could be accomplished in the future by chemical (e.g., NaOH) or enzyme (e.g., purified IcaB or PgaB) treatment. Other adjustable parameters that could potentially impact the immunogenicity of our glycOMVs include (*i*) dosage, which likely could be increased without adverse effects given the dramatically reduced pyrogenicity of our detoxified OMVs (21), and (*ii*) addition of an adjuvant, such as alum, which was not included in any of our OMV immunizations but is a key component of Bexsero, a licensed OMV-containing vaccine (16).

In regard to clinical development of PNAG-based and OMV-based immunotherapies and vaccines for humans, there are two important issues to consider: (*i*) that functional antibody to PNAG could disrupt the normal PNAG-producing microbiota present in the gastrointestinal or female genital tract and on the skin and (*ii*) that the lipid A portion of LPS, known as endotoxin, in OMVs may contribute to lethal septic shock at high levels (43). The concern about negative consequences arising from disruption of commensal organisms can be allayed by several observations (ref. 5 has a detailed discussion). First, there were no signs or symptoms associated with the commensal microbiota during phase I clinical trials of mAb F598 in humans (44). Second, ∼5% of healthy humans develop natural opsonic/protective antibody to PNAG (38), indicating that such antibodies do little to upset the overall health of these individuals. Third, the effect of the immune system on shaping and controlling microbiota composition and diversity is well-established (45). For example, antibodies to resident microbial antigens dominate our natural immune responses, and adaptive immune responses against the normal commensal microbiota are an integral component of mucosal immunity (46). Because immunization against PNAG would only increase the levels of antibody to resident microbes by a few 10ths of a percent, the effect of vaccine-induced anti-PNAG antibodies is likely to be dwarfed by the rest of the natural and protective antibodies to commensal microbial antigens.

Concerns about OMV toxicity can similarly be allayed by several observations. First, the efficacy, tolerability, and safety of native OMVs derived from *N. meningitidis* in humans are well-proven (14, 16, 47). Second, endotoxin removal is possible by either chemically stripping away LPS from OMVs through the use of polymyxin B columns (15, 17) or genetically engineering the host strain with mutations (e.g., *lpxM* knockout) that remodel lipid A to yield a pentaacylated variant that is significantly less toxic, as measured by hTLR4 activation, while still retaining desirable immunomodulatory qualities (21). Here, detoxified rdPNAG-glycOMVs with pentaacylated lipid A elicited rPNAG-specific antibodies and protected mice at levels that were indistinguishable from rdPNAG-glycOMVs bearing wild-type hexaacylated lipid A. Overall, the results from this study represent a promising proof of concept for the use of engineered glycOMV vaccines targeting PNAG as a route to clearing infection by diverse human and animal pathogens that are susceptible to killing by this humoral immune factor.

Materials and Methods

Bacterial Strains, Growth, and Plasmids. All OMV production involved the hypervesiculating *E. coli* strain JC8031, which lacks the *tolRA* genes (22), or its isogenic derivatives. Specifically, JH8033 is a Δ*lpxM* derivative of JC8031 that produces less reactogenic OMVs due to pentaacylation of its lipid A (21). Strains JC8031 Δ*pgaC* and JH8033 Δ*pgaC* were generated from JC8031 and JH8033, respectively, using P1 transduction of the *pgaC*::kan allele derived from the Keio collection (48). The *E. coli* Top10 strain was used for crude preparation of PNAG. *S. aureus* CP8 strain MN8 and *S. aureus* strain Rosenbach (ATCC 29213), both known producers of PNAG, were used for opsonic killing and mouse challenge experiments, respectively. *F. tularensis* strains evaluated for surface expression of PNAG were *F. tularensis* subsp. *holarctica*, *F. tularensis* subsp. *novicida* U112, and *F. tularensis* subsp. *tularensis* Schu S4. *F. tularensis* subsp. *holarctica* LVS Iowa (ATCC 29684) was used for SBA and mouse challenge studies and was originally provided by Karen Elkins, US Food and Drug Administration, Rockville, MD. The strain designation of LVS isolates was confirmed by the absence of *pdpD*, the absence of *pilA*, and the deletion in the C terminus of FTT0918 (49).

All *E. coli* strains in this study were grown in LB media (10 g/L tryptone, 10 g/L NaCl, 5 g/L yeast extract) or on LB agar (LBA) plates. *S. aureus* strains were cultured in tryptic soy broth (TSB) or on TSB agar supplemented with 5% sheep's blood. *F. tularensis* strains were cultured in modified Mueller Henton broth supplemented with 2% IsoVitaleX (BD Biosciences) or on cysteine heart agar (Thermo-Fisher) supplemented with 9% sheep's blood. All bacterial strains were grown at 37 °C in media supplemented with appropriate antibiotics for plasmid and strain selection unless stated otherwise. All reagents were purchased from Sigma-Aldrich unless stated otherwise.

Overexpression of the *E. coli pga* operon was achieved using plasmid pUCP18Tc-*pga* (25), a high-copy number plasmid that enables isopropyl β-D-1-thiogalactopyranoside (IPTG)-inducible expression of *pgaABCD* as a single transcript. The gene encoding the *S. aureus* PNAG deacetylase IcaB was PCR amplified from genomic DNA using primers IcaB_F (5′-ACCATGGGAAAAAAGATTTGGCTGGCGCTGGCTGGTTTAGTTTTAGCGTTTAGCGCATCGGCGGATGACGATTCACCTAAAAAACTGAAA-3′) and IcaB_R (5′-ACTGCAGTTAATGGTGGTGGTGATGATGGCTACCGCTGCCGCTACCATCTTTTTCATGGAATCCGTCCCATCTC-3′), which replaced the native signal peptide of IcaB with an *E. coli* DsbA signal peptide for periplasmic targeting and introduced a C-terminal Gly_3Ser linker followed by a 6×-His tag for immunodetection. The PCR-amplified product was digested using NcoI and PstI enzymes and ligated into identical sites in plasmid pTrc99A (Amersham Pharmacia), yielding pTrc-IcaB for IPTG-inducible expression of IcaB.

OMV Preparation. OMVs were prepared as described previously (18) using JC8031 or its isogenic derivatives with or without plasmids pUCP18Tc-*pga* and/or pTrc-IcaB. Cells were selected on LBA supplemented with the appropriate antibiotic as needed, from which single colonies were selected and grown overnight in liquid LB media. Saturated cultures were subcultured 1:100 in LB supplemented with appropriate antibiotics and grown to midlog phase (OD_{600} ∼ 0.6), at which point *pgaABCD* and/or *icaB* expression was induced with 0.1 mM IPTG for 16–20 h at 37 °C. Cells were pelleted via centrifugation at 10,000 × *g* for 10 min. Cell-free culture supernatants were collected postinduction and filtered through a 0.2-μm filter. OMVs were isolated by ultracentrifugation (TiSW28 rotor; Beckman-Coulter) at 141,000 × *g* for 3 h at 4 °C and resuspended in sterile PBS. OMVs were quantified by the bicinchoninic acid (BCA) total protein assay (Pierce) using BSA as the protein standard. OMVs were subjected to density gradient ultracentrifugation as described previously (18, 20, 21) and in *SI Appendix, SI Materials and Methods*.

Dot Blot, SDS/PAGE, and Western Blot Analysis. For dot blot analysis, OMV-containing fractions were diluted to 200 μg/mL total protein in PBS and incubated with or without 50 μg/mL dispersin B (Kane Biotech, Inc.) at 37 °C for 24 h. Samples were spotted directly onto nitrocellulose membranes followed by blocking with 5% milk in Tris-buffered saline (TBS) and probing with antibodies as described below for Western blot analysis. For SDS/PAGE, OMV-containing fractions were boiled for 15 min in loading buffer containing β-mercaptoethanol. After cooling to room temperature, samples were loaded into 12% polyacrylamide gels (BioRad) and separated electrophoretically. To visualize proteins, SDS/PAGE gels were stained with Coomassie Brilliant Blue R-250 (BioRad). For Western blot analysis, subcellular fractions, including soluble periplasm, whole-cell lysate, and OMV fractions,

were separated by SDS/PAGE as described above and subsequently transferred to a PVDF membrane via semidry transfer. Membranes were blocked with 5% milk in TBS and then probed with the following primary antibodies: HRP-conjugated mouse anti-His antibody (Abcam) for the detection of IcaB, human mAb F598 for the detection of PNAG and dPNAG, and mouse anti-OmpA. Anti-human and anti-mouse HRP-conjugated secondary antibodies (Promega) were used in combination with mAb F598 and anti-OmpA, respectively. Signals were visualized using HRP substrate Clarity ECL (BioRad) and were imaged with a ChemiDoc XRS+ Imaging System (BioRad). Structural analysis of vesicles was performed via TEM as described previously (17) and in *SI Appendix, SI Materials and Methods*. Confocal microscopy and immunochemical detection of PNAG are also described in *SI Appendix, SI Materials and Methods*.

Purification of rPNAG from *E. coli*. Top10 *E. coli* cells, which do not natively produce PNAG, were transformed with pUCP18Tc-*pga* and cultured to midlog phase. Production of rPNAG was stimulated with IPTG, and the cells were cultured for an additional 16 h, after which they were pelleted via centrifugation at 10,000 × *g* for 10 min. The supernatant was recovered and filtered through a 0.2-μm filter before being concentrated 25× in a 3-kDa molecular weight cutoff concentration column (Millipore). rPNAG was then precipitated from solution via the addition of 2 vol of ethanol. Insoluble rPNAG was recovered by gentle centrifugation (<1,000 × *g* for <5 min), and the supernatant was discarded. The pelleted rPNAG was resuspended in PBS (1:50 original supernatant volume) and incubated overnight in 10 μg/mL lysozyme and 10 μg/mL DNaseI at 37 °C. The peptidoglycan- and DNA-digested rPNAG was then subjected to 100 μg/mL proteinase K (Promega) treatment overnight at 37 °C. The isolated rPNAG was then dialyzed into water to remove digested peptides and nucleotides using a 5-kDa Slide-A-Lyzer cassette (Thermo-Fisher) before being lyophilized. The purity of this sample was evaluated using a Bradford total protein assay and was determined to have <1% contaminating protein by mass. The method of purification of PNAG from the *S. aureus* MN8m strain and the chemical characterization of the resulting PNAG antigen were performed as described previously (34) and in *SI Appendix, SI Materials and Methods*.

ELISA. PNAG-specific antibodies produced in immunized mice were measured via indirect ELISA using a modification of a previously described protocol (17). Briefly, sera were isolated from the collected blood draws after centrifugation at 2,200 × *g* for 10 min and stored at −20 °C; 96-well plates (Maxisorp; Nunc Nalgene) were coated with purified rPNAG (25 μg/mL in PBS, pH 7.4) and incubated overnight at 4 °C. The next day, plates were washed three times with PBST (PBS, 0.05% Tween-20, 0.3% BSA) and blocked overnight at 4 °C with 5% nonfat dry milk (Carnation) in PBS. Samples were serially diluted by a factor of five in triplicate between 1:100 and 1:7,812,500 in blocking buffer and added to the plate for 2 h at 37 °C. Plates were washed three times with PBST and incubated for 1 h at 37 °C in the presence of one of the following HRP-conjugated antibodies (all from Abcam and used at 1:10,000 dilution): goat anti-mouse IgG, anti-mouse IgG1, anti-mouse IgG2a, anti-mouse IgA, and anti-mouse IgM. After three additional washes with PBST, 3,3′-5,5′-tetramethylbenzidine substrate (1-Step Ultra TMB-ELISA; Thermo-Fisher) was added, and the plate was incubated at room temperature for 30 min. The reaction was halted with 2 M H_2SO_4, and absorbance was quantified via microplate spectrophotometer (Molecular Devices) at a wavelength of 450 nm. Serum antibody titers were determined by measuring the lowest dilution that resulted in signal 3 SDs above no serum background controls. Statistical significance was determined using ANOVA and the Tukey–Kramer post hoc honest significant difference test and compared against the PBS and empty OMV control cases. OmpA-specific serum IgG antibodies were measured in a similar way with the following modifications: purified OmpA (ProSpec) was coated on high-binding 96-well plates (Corning), and sera from individual mice in each group were pooled and serially diluted by a factor of 10 in triplicate from 1:100.

Opsonization Phagocytosis and Killing Assay. Opsonization phagocytosis and killing assay was performed as described previously using *S. aureus* CP8 strain MN8 (6). Bacteria were grown overnight on tryptic soy blood agar and suspended to a final concentration of 2 × 10^7 cfu/mL in sterile gelatin veronal buffer (GVB; Boston BioProducts). Serum samples taken 10 wk after immunization from unchallenged mice were heat inactivated via incubation at 56 °C for 30 min before use. Human mAb F598 to PNAG was used as a positive control for bactericidal activity, while mAb F429 to *P. aeruginosa* alginate was used as a negative control. Serum samples and mAbs were diluted 1:30 in sterile GVB and then serially diluted twofold to a maximum dilution factor of 1:120 (10 μg/mL = 1:30 dilution of mAbs). Neutrophils were isolated from donor blood samples using the EasySep magnetic isolation kit (StemCell) and suspended to a final concentration of 10^7 cells per 1 mL in GVB. Serum was also isolated from donor blood via centrifugation at 2,200 × *g* for 10 min to obtain autologous complement for use in the assay. Complement was diluted to 40% (vol/vol) in GVB and adsorbed to *S. aureus* MN8 at a final concentration of ∼10^9 cfu/mL for 30 min at 4 °C to remove any PNAG binding antibodies from the complement. Adsorbed complement was sterilized through a 0.5-μm filter and stored on ice before use. A fraction of adsorbed complement was heat inactivated at 56 °C for 30 min to serve as a control. Equal volumes (100 μL) of serum, complement, neutrophils, and bacterial dilution were combined and mixed end-over-end in 2.0-mL round-bottom microcentrifuge tubes for 3 h at 37 °C. Samples were diluted 1:10 and 1:100 in TBS with 0.05% Tween, and 10 μL of each dilution was spotted in duplicate on plates and allowed to trail down one-half the length of the plate to facilitate colony counting. Plates were then incubated overnight at 37 °C, and colonies were counted the next day. Percentage of bactericidal activity was calculated by comparing the mean number of cfu in an experimental group with the number of cfu determined for the mAb F429 control. Values were reported as averages of bactericidal activity from individual mice in each immunization group, and the error bars are the SD.

SBA. SBA was performed using a modified version of previously reported protocols (5, 50). An overnight culture of *F. tularensis* LVS Iowa was used to make a suspension of 10^5 cfu/mL in sterile PBS. Serum samples taken 10 wk after immunization from unchallenged mice were heat inactivated via incubation at 56 °C for 30 min before use. Human mAb F598 (1 mg/mL = 1:1 dilution of mAb) was used as a positive control for bactericidal activity. Serum samples and mAb F598 were diluted 1:2 in sterile PBS and then serially diluted threefold to a maximum dilution factor of 1:54 before being diluted 1:5 in the assay (final concentration range 1:10–1:270). Naïve baby rabbit complement (Cedarlane) or heat-inactivated complement (56 °C for 30 min) was used at a final concentration of 6% (vol/vol). Reactions were incubated at 37 °C for 30 min before 10 μL of each reaction was spotted on cysteine heart agar + 9% sheep's blood and allowed to trail down one-half the length of the plate to facilitate colony counting. Plates were then incubated overnight at 37 °C, and colonies were counted the next day. Percentage of bactericidal activity was calculated by comparing the number of cfu in a spot with the number of cfu in the spot of the "no complement" control. Values shown are averages of bactericidal activity from individual mice in each immunization group, and the error bars are the SD.

Mouse Immunizations and Pathogen Challenge. Four-week-old female BALB/c mice (Jackson Lab) were immunized s.c. with 100-μL injections of PBS (pH 7.4), and rPNAG purified from *E. coli* Top10 cells carrying plasmid pUCP18Tc-*pga*, 5GlcNH$_2$-TT conjugate, or one of the OMV formulations. Each dose represented 10 μg of material as determined by total mass in the case of purified rPNAG or total protein content as determined by BCA in all other cases. The purified rPNAG and 5GlcNH$_2$-TT conjugate were formulated with incomplete Freund's adjuvant (50% vol/vol). Mice were boosted at 3 wk and again at 6 wk with the same doses. Blood was collected from each mouse from the mandibular sinus before each immunization and immediately before challenge. At 56 d after the initial immunization, each group was challenged with 1 × 10^9 cfu/mL (10 × mLD$_{50}$) of *S. aureus* strain Rosenbach in 200 μL sterile PBS via tail vein injection. Determination of mLD$_{50}$ for *S. aureus* strain Rosenbach via tail vein injection is described in *SI Appendix, SI Materials and Methods*. Mice were weighed thrice daily for the first 72 h and then once daily for the remaining 4 d. Mice were euthanized if their weight dropped below 80% of weight at t = 0 or if they became moribund. After 7 d, a Kaplan–Meier plot was generated. Statistical significance was determined using a log rank test compared with survival of the PBS and empty OMV control groups. The protocol number for these animal trials was 2012–0132, and they were approved by the Institutional Animal Care and Use Committee at Cornell University.

Challenge against *F. tularensis* subsp. *holarctica* LVS was performed as described previously (21). Briefly, groups of five 6- to 8-wk old female BALB/c mice (National Cancer Institute) were each immunized i.p. with 100-μL injections of PBS (pH 7.4), 5GlcNH$_2$-TT conjugate, detoxified empty OMVs, or detoxified rdPNAG-glycOMVs. The mice were boosted with the same doses at day 14 and again at day 28. At 70 d after the initial immunization, each group was challenged i.p. with 500 cfu (∼500 × LD$_{50}$) of *F. tularensis* LVS Iowa. The health of the mice was examined daily for signs of disease. When an animal became moribund, it was killed according to the procedure in the approved protocol. Mice were monitored until 14 d, at which time a Kaplan–Meier plot was generated. Statistical significance was determined using a log rank test compared with survival of the PBS and detox empty OMV control groups. The

protocol number for the animal studies was 1305086, and they were approved by the University of Iowa Animal Care and Use Committee.

ACKNOWLEDGMENTS. We thank Roland Lloubes, Karen Elkins, and Wilfred Chen for strains and antibodies used in this work. We acknowledge the use of the Cornell Center for Materials Research Shared Facilities, which are supported through National Science Foundation (NSF) Materials Research Science and Engineering Center Program DMR-1120296. This material was based on work supported by NSF Graduate Research Fellowships (to T.C.S. and K.B.W.); Samuel C. Fleming Family Graduate Research Fellowships (to T.D.M. and K.B.W.); NIH Grants EB005669-01 (to D.P. and M.P.D.), AI044642 (to B.D.J.), AI057160 (to B.D.J.), EY016144 (to G.B.P.), and GM088905-01 (to M.P.D.); Project 14 of the Midwest Regional Center of Excellence for Biodefense and Emerging Infectious Disease Research (B.D.J.); and NSF Grants CBET-1159581 (to M.P.D.) and CBET-1264701 (to M.P.D.). This work was also supported by unrestricted support from Alopexx Vaccine, LLC (C.C.-B.).

1. Whitfield C (2006) Biosynthesis and assembly of capsular polysaccharides in Escherichia coli. *Annu Rev Biochem* 75:39–68.
2. Raetz CR, Whitfield C (2002) Lipopolysaccharide endotoxins. *Annu Rev Biochem* 71: 635–700.
3. Heilmann C, et al. (1996) Molecular basis of intercellular adhesion in the biofilm-forming Staphylococcus epidermidis. *Mol Microbiol* 20:1083–1091.
4. Wang X, Preston JF, 3rd, Romeo T (2004) The pgaABCD locus of Escherichia coli promotes the synthesis of a polysaccharide adhesin required for biofilm formation. *J Bacteriol* 186:2724–2734.
5. Cywes-Bentley C, et al. (2013) Antibody to a conserved antigenic target is protective against diverse prokaryotic and eukaryotic pathogens. *Proc Natl Acad Sci USA* 110: E2209–E2218.
6. Maira-Litrán T, Kropec A, Goldmann DA, Pier GB (2005) Comparative opsonic and protective activities of Staphylococcus aureus conjugate vaccines containing native or deacetylated staphylococcal poly-N-acetyl-beta-(1-6)-glucosamine. *Infect Immun* 73: 6752–6762.
7. Cerca N, et al. (2007) Molecular basis for preferential protective efficacy of antibodies directed to the poorly acetylated form of staphylococcal poly-N-acetyl-beta-(1-6)-glucosamine. *Infect Immun* 75:3406–3413.
8. Gening ML, et al. (2010) Synthetic beta-(1->6)-linked N-acetylated and nonacetylated oligoglucosamines used to produce conjugate vaccines for bacterial pathogens. *Infect Immun* 78:764–772.
9. Astronomo RD, Burton DR (2010) Carbohydrate vaccines: Developing sweet solutions to sticky situations? *Nat Rev Drug Discov* 9:308–324.
10. Frasch CE (2009) Preparation of bacterial polysaccharide-protein conjugates: Analytical and manufacturing challenges. *Vaccine* 27:6468–6470.
11. Seale A, Finn A (2011) What is the best way to use conjugate vaccines? *Curr Opin Infect Dis* 24:219–224.
12. Kulp A, Kuehn MJ (2010) Biological functions and biogenesis of secreted bacterial outer membrane vesicles. *Annu Rev Microbiol* 64:163–184.
13. Alaniz RC, Deatherage BL, Lara JC, Cookson BT (2007) Membrane vesicles are immunogenic facsimiles of Salmonella typhimurium that potently activate dendritic cells, prime B and T cell responses, and stimulate protective immunity in vivo. *J Immunol* 179:7692–7701.
14. Sanders H, Feavers IM (2011) Adjuvant properties of meningococcal outer membrane vesicles and the use of adjuvants in Neisseria meningitidis protein vaccines. *Expert Rev Vaccines* 10:323–334.
15. Ellis TN, Leiman SA, Kuehn MJ (2010) Naturally produced outer membrane vesicles from Pseudomonas aeruginosa elicit a potent innate immune response via combined sensing of both lipopolysaccharide and protein components. *Infect Immun* 78: 3822–3831.
16. Gorringe AR, Pajón R (2012) Bexsero: A multicomponent vaccine for prevention of meningococcal disease. *Hum Vaccin Immunother* 8:174–183.
17. Chen DJ, et al. (2010) Delivery of foreign antigens by engineered outer membrane vesicle vaccines. *Proc Natl Acad Sci USA* 107:3099–3104.
18. Kim JY, et al. (2008) Engineered bacterial outer membrane vesicles with enhanced functionality. *J Mol Biol* 380:51–66.
19. Rappazzo CG, et al. (2016) Recombinant M2e outer membrane vesicle vaccines protect against lethal influenza A challenge in BALB/c mice. *Vaccine* 34:1252–1258.
20. Valentine JL, et al. (2016) Immunization with outer membrane vesicles displaying designer glycotopes yields class-switched, glycan-specific antibodies. *Cell Chem Biol* 23:655–665.
21. Chen L, et al. (2016) Outer membrane vesicles displaying engineered glycotopes elicit protective antibodies. *Proc Natl Acad Sci USA* 113:E3609–E3618.
22. Bernadac A, Gavioli M, Lazzaroni JC, Raina S, Lloubès R (1998) Escherichia coli tol-pal mutants form outer membrane vesicles. *J Bacteriol* 180:4872–4878.
23. Choi AH, Slamti L, Avci FY, Pier GB, Maira-Litrán T (2009) The pgaABCD locus of Acinetobacter baumannii encodes the production of poly-beta-1-6-N-acetylglucosamine, which is critical for biofilm formation. *J Bacteriol* 191:5953–5963.
24. Wang X, et al. (2005) CsrA post-transcriptionally represses pgaABCD, responsible for synthesis of a biofilm polysaccharide adhesin of Escherichia coli. *Mol Microbiol* 56: 1648–1663.
25. Roux D, et al. (2015) Identification of poly-N-acetylglucosamine as a major polysaccharide component of the Bacillus subtilis biofilm matrix. *J Biol Chem* 290: 19261–19272.
26. Manuel SG, et al. (2007) Role of active-site residues of dispersin B, a biofilm-releasing beta-hexosaminidase from a periodontal pathogen, in substrate hydrolysis. *FEBS J* 274:5987–5999.
27. Fazekas E, Kandra L, Gyémánt G (2012) Model for β-1,6-N-acetylglucosamine oligomer hydrolysis catalysed by DispersinB, a biofilm degrading enzyme. *Carbohydr Res* 363: 7–13.
28. Balsalobre C, et al. (2006) Release of the type I secreted alpha-haemolysin via outer membrane vesicles from Escherichia coli. *Mol Microbiol* 59:99–112.
29. Pier GB, et al. (2004) Human monoclonal antibodies to Pseudomonas aeruginosa alginate that protect against infection by both mucoid and nonmucoid strains. *J Immunol* 173:5671–5678.
30. Bogaert D, Hermans PW, Adrian PV, Rümke HC, de Groot R (2004) Pneumococcal vaccines: An update on current strategies. *Vaccine* 22:2209–2220.
31. Cerca N, et al. (2007) Protection against Escherichia coli infection by antibody to the Staphylococcus aureus poly-N-acetylglucosamine surface polysaccharide. *Proc Natl Acad Sci USA* 104:7528–7533.
32. Needham BD, et al. (2013) Modulating the innate immune response by combinatorial engineering of endotoxin. *Proc Natl Acad Sci USA* 110:1464–1469.
33. Fortier AH, Slayter MV, Ziemba R, Meltzer MS, Nacy CA (1991) Live vaccine strain of Francisella tularensis: Infection and immunity in mice. *Infect Immun* 59:2922–2928.
34. Maira-Litrán T, et al. (2002) Immunochemical properties of the staphylococcal poly-N-acetylglucosamine surface polysaccharide. *Infect Immun* 70:4433–4440.
35. Price NL, et al. (2016) Glycoengineered outer membrane vesicles: A novel platform for bacterial vaccines. *Sci Rep* 6:24931.
36. Zhang F, Lu YJ, Malley R (2013) Multiple antigen-presenting system (MAPS) to induce comprehensive B- and T-cell immunity. *Proc Natl Acad Sci USA* 110:13564–13569.
37. Thanawastien A, Cartee RT, Griffin TJ, 4th, Killeen KP, Mekalanos JJ (2015) Conjugate-like immunogens produced as protein capsular matrix vaccines. *Proc Natl Acad Sci USA* 112:E1143–E1151.
38. Skurnik D, et al. (2012) Natural antibodies in normal human serum inhibit Staphylococcus aureus capsular polysaccharide vaccine efficacy. *Clin Infect Dis* 55:1188–1197.
39. Fulop M, Mastroeni P, Green M, Titball RW (2001) Role of antibody to lipopolysaccharide in protection against low- and high-virulence strains of Francisella tularensis. *Vaccine* 19:4465–4472.
40. Proctor RA (2012) Challenges for a universal Staphylococcus aureus vaccine. *Clin Infect Dis* 54:1179–1186.
41. Karauzum H, Datta SK (2016) Adaptive immunity against Staphylococcus aureus. *Curr Top Microbiol Immunol* 409:419–439.
42. Schaub B, et al. (2004) TLR2 and TLR4 stimulation differentially induce cytokine secretion in human neonatal, adult, and murine mononuclear cells. *J Interferon Cytokine Res* 24:543–552.
43. Raetz CRH, et al. (2009) Discovery of new biosynthetic pathways: The lipid A story. *J Lipid Res* 50(Suppl):S103–S108.
44. Vlock D, Lee JC, Kropec-Huebner A, Pier GB (2010) Pre-clinical and initial phase I evaluations of a fully human monoclonal antibody directed against the PNAG surface polysaccharide on *Staphylococcus aureus*. *Abstracts of the 50th Interscience Conference on Antimicrobial Agents and Chemotherapy 2010* (Am Soc Microbiol, Washington, DC), G1-1654/329 (abstr).
45. Hooper LV, Littman DR, Macpherson AJ (2012) Interactions between the microbiota and the immune system. *Science* 336:1268–1273.
46. Hand TW, et al. (2012) Acute gastrointestinal infection induces long-lived microbiota-specific T cell responses. *Science* 337:1553–1556.
47. Holst J, et al. (2009) Properties and clinical performance of vaccines containing outer membrane vesicles from Neisseria meningitidis. *Vaccine* 27:B3–B12.
48. Baba T, et al. (2006) Construction of Escherichia coli K-12 in-frame, single-gene knockout mutants: The Keio collection. *Mol Syst Biol* 2:2006.0008.
49. Griffin AJ, Crane DD, Wehrly TD, Bosio CM (2015) Successful protection against tularemia in C57BL/6 mice is correlated with expansion of Francisella tularensis-specific effector T cells. *Clin Vaccine Immunol* 22:119–128.
50. Sebastian S, et al. (2007) A defined O-antigen polysaccharide mutant of Francisella tularensis live vaccine strain has attenuated virulence while retaining its protective capacity. *Infect Immun* 75:2591–2602.